INTERNATIONAL JOURNAL OF CLIMATOLOGY
Int. J. Climatol. **37**: 4576–4585 (2017)
Published online 22 May 2017 in Wiley Online Library
(wileyonlinelibrary.com) DOI: 10.1002/joc.5106

The relation of cross-equatorial flow during winter and spring with South China Sea summer monsoon onset

Ailan Lin,[a*] Renhe Zhang[b,c] and Chao He[a]
[a] *Institute of Tropical and Marine Meteorology/Guangdong Provincial Key Laboratory of Regional Numerical Weather Prediction, China Meteorological Administration, Guangzhou, China*
[b] *Institute of Atmospheric Sciences, Fudan University, Shanghai, China*
[c] *CAS Center for Excellence in Tibetan Plateau Earth Sciences, Beijing, China*

ABSTRACT: The relationship between cross-equatorial flow (CEF) during winter and spring and the South China Sea summer monsoon (SCSSM) onset is investigated by data diagnoses for the period of 1979–2013 and numerical experiments. The SCSSM onset is found to have a significant negative correlation with the CEF nearby the Philippines in preceding January, February and March prior to SCSSM onset. A strong CEF during January, February and March tends to be succeeded by an early onset of SCSSM, whereas a weak CEF is likely to be followed by a late onset. The CEF in preceding months links with the SCSSM onset through the subtropical high over South China Sea and western North Pacific in April. The subtropical high in April is weak and eastward shifted (strong and westward shifted) when the CEF in preceding months is strong (weak). The weak and eastward shifted (strong and westward shifted) subtropical high favours (does not favour) the convection developing (depressing) over South China Sea, resulting in an early (late) onset of SCSSM. The anomalies of CEF nearby the Philippines in preceding months and its close relationship with subsequent subtropical high are caused by the sea surface temperature anomalies (SSTA) and atmospheric heating source over tropical western Pacific. The difference of SSTA between south and north of equator in tropical western Pacific and the corresponding atmospheric diabatic heating result in the anomalies of CEF in January, February and March, and impact the activity of subtropical high in April. The positive SSTA in tropical western Pacific, combining with the wet and warm climatic background over northern South China Sea and coastal areas of Southern China in April are favourable for a cyclonic circulation anomaly occurring over northern South China Sea. As a result, the subtropical high is weak and eastward shifted, and the SCSSM onset is early.

KEY WORDS cross-equatorial flow; South China Sea summer monsoon onset; atmospheric heating source; sea surface temperature anomalies

Received 14 October 2016; Revised 7 March 2017; Accepted 28 March 2017

1. Introduction

Cross-equatorial flow (CEF) plays a key role in transporting mass, momentum, heat, moisture between Southern and Northern Hemisphere. CEF is one of the important factors which reflect and influence the weather and climate over the Southern and Northern Hemisphere. Much has been learned about the characteristics and dynamics of CEF since Findlater (1969) found the Somali low-level jet (Krishnamurti *et al.*, 1976; Tang *et al.*, 1985; Qian *et al.*, 1987; Rodwell and Hoskins, 1995; Liu *et al.*, 2009; Zeng *et al.*, 2011). CEF is one of the main components in Asian monsoon system, and is related closely with Asian climate. Therefore, much attention has been paid on impacts of CEF on Asian summer monsoon (Chen *et al.*, 2000; Li and Wu, 2002; Ding and He, 2006; Gao and Xue, 2006; Qiu and Sun, 2013), rainfall over China (Li *et al.*, 2000; Wang and Xue, 2003; Lei and Yang, 2008; Zhu, 2012; Li and Li, 2014), and weather systems, such as subtropical high over western North Pacific (Bi *et al.*, 2004; Xu *et al.*, 2006; Lin *et al.*, 2007), Typhon (Wang and Leftwich, 1984; Huang *et al.*, 2008; Feng *et al.*, 2014), etc. CEF over Western Hemisphere is related closely with distribution of seasonal rainfall over its adjacent area as well as over Eastern Hemisphere (Wang and Fu, 2002). It is thus clear that CEF has important indication for Asian monsoon circulation, weather, and climate.

The South China Sea summer monsoon (SCSSM) onset is the commencement of East Asian summer monsoon and rainy season over East Asia. The interannual variability of SCSSM onset is significant. For example, the difference of date between the earliest onset and the latest onset during the past 35 years is more than 50 days (Lin *et al.*, 2013). Consequently, the study on the mechanism of SCSSM onset attracts a great attention. It has been proved that the SCSSM onset is related closely to sea surface temperature anomalies (SSTA) inside and outside tropics (e.g. Ding and Li, 1999; Ding *et al.*, 2002; Mao *et al.*, 2000; Zhao *et al.*, 2000; Huang *et al.*, 2006; Liang *et al*, 2006; Lin *et al.*, 2013). Some research also shows

* Correspondence to: A. Lin, Institute of Tropical and Marine Meteorology, 312 Dongguanzhuang Road, Guangzhou 510640, China. E-mail: allin@grmc.gov.cn

that cold air from Southern Hemisphere and the CEF influence monsoon activity. For example, it has been demonstrated that cold air from Southern Hemisphere triggers the onset and evolution of summer monsoon over Northern Hemisphere (Kuettner and Unninayar, 1980; Sikka, 1980; Tao *et al.*, 1983), and circulation variation over Southern Hemisphere can break off Northern summer monsoon as well (Ramaswamy and Pareek, 1978; Rodwell, 1997). Studies by He and Chen (1989) and He *et al.* (1991) indicated that the 40-day oscillation achieves the impact of old air from Southern Hemisphere on the summer monsoon in East Asia, and the CEF plays a key role in the interaction between Southern and Northern Hemisphere. Setting up of Somali CEF leads to the reinforcing and expanding eastward of westerlies over equatorial Indian Ocean, and results in the onset of SCSSM ultimately (Li and Wu, 2002). Two pentads prior to SCSSM onset, Somali CEF intensifies rapidly, CEF around South China Sea enhances quickly and pushes subtropical high northward in the same time, then the SCSSM onset is promoted jointly (Gao and Xue, 2006).

The previous studies focus mainly on the imminent impact of CEF on the SCSSM onset. Few investigations have been documented on the influence of CEF in preceding winter or spring on the SCSSM onset. The objective of this study is therefore to analyse the relationship between the SCSSM onset and the CEF in preceding winter and spring, and to understand whether the prior CEF variability is a precursor for the subsequent SCSSM onset. We intend to provide new information for short-term climate prediction of SCSSM onset. In Section 2 the data and methods used in this study are introduced. The relations of CEF in preceding winter and spring with SCSSM onset and their physical linkage are discussed in Sections 3 and 4, respectively. Conclusions and discussions are given in Section 5.

2. Data and methods

The daily and monthly mean meteorological data used in the present study are from National Center for Environmental Prediction/Department of Energy (NCEP–DOE) Reanalysis 2 (Kanamitsu *et al.*, 2002), with a global coverage at a 2.5° × 2.5° resolution. The monthly sea surface temperature (SST) at a 2° × 2° resolution is from NOAA ERSST.v2 (Smith and Reynolds, 2004). The data period is from 1979 to 2013.

The CEF intensity in the present study is defined as the meridional winds at 850 hPa averaged along equator over 5°S–5°N. According to Lin *et al.* (2013, 2016), the SCSSM onset date is taken to be the first day that the steady westerly winds at 850 hPa establish over the South China Sea region (105°–120°E,5°–20°N). According to this index, the climatological onset date of SCSSM in past 35 years is 16 May (Lin *et al.*, 2013).

The apparent heat source Q_1 (Yanai *et al.*, 1973) which depicts the diabatic heating of atmosphere is computed by

$$Q_1 = C_p \left[\frac{\partial T}{\partial t} + V \cdot \nabla T + \left(\frac{p}{p_0} \right)^k \omega \frac{\partial \theta}{\partial p} \right]$$

where T is air temperature, ω the vertical p-velocity, $p_0 = 1000$ hPa, θ the potential temperature, $R = 287$ J/(kg · K), $Cp = 1005$ J/(kg · K), $k = R/Cp \approx 0.286$. Heating rate can be obtained from $Q1/Cp$ (K/s). Monthly mean of heating rate is computed based on the daily value.

In order to investigate the response of circulation to anomalous heating, a dry version AGCM developed by Geophysical Fluid Dynamics Laboratory (GFDL) (Jiang and Li, 2005) is adopted, and is referred to as GFDL_dry model hereafter. The GFDL_dry model has a spectral dynamic core with triangular truncation of 42 wave numbers (T42). It has five vertical levels at sigma coordinate, ranging from sigma = 0.1 to sigma = 0.9. This model was widely used by previous studies in East Asia-West Pacific region (e.g. Wang *et al.*, 2012; Wei *et al.*, 2014, 2015; Leung *et al.*, 2016).

In exploring the atmospheric response to prescribed SSTA, the Community Atmosphere Model version 4 (CAM4; Neale *et al.*, 2010) was also used in this study. The CAM4 adopts a finite-volume dynamic core with a horizontal resolution of about 1.9° in latitude and 2.5° in longitude. It has a hybrid sigma-pressure coordinate with 26 vertical levels. A control experiment (CTL) was run for 30 years, forced by the climatological annual cycle of SST and sea ice concentration (Hurrell *et al.*, 2008). The sensitivity experiments are done by modifying the SST field, and are also run for 30 years. The last 25 years of each experiment are analysed, and each year can be treated as an ensemble member. The composite differences between the sensitivity runs and CTL run are illustrated, to reveal the atmospheric response to the prescribed SST anomalies.

3. Correlation between CEF in preceding winter and spring and SCSSM onset

The SCSSM onset date during past 35 years changes between the 4th pentad in April and 2nd pentad in June (Lin *et al.*, 2013). Here we focus the possible linkage between CEF in winter and early spring (December to March) before SCSSM onset and the date of SCSSM onset. Figure 1 shows the correlation coefficients between SCSSM onset date and CEF in preceding months from December to March. It is shown that the CEF nearby the Philippines (120°–130°E) is related significantly with SCSSM onset date in January, February and March. The significant negative correlation lasts three successive months. Correlation coefficient between composite intensity of CEF from January to March and the onset date reaches −0.58, exceeding 99.9% confidence level. As seen from Figure 2, it is clear that the composite intensity anomalies varies reversely with the onset date anomalies, indicating a strong (weak) composite intensity of CEF nearby the Philippines in preceding months corresponds to an early (late) onset of the SCSSM.

Note that the intensity of CEF is expressed by the merridional winds at 850 hPa. The climatological CEF is northerlies in January, February, and March, and its

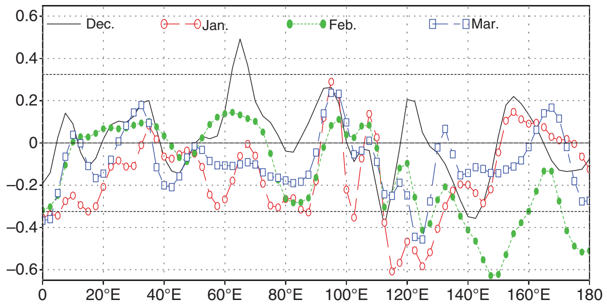

Figure 1. Zonal distribution of correlation coefficients between SCSSM onset date and meridional winds at 850 hPa over equator (5°S–5°N) preceding the onset date in December (line), January (hollow circle), February (solid circle), and March (square). The black dashed lines indicate the threshold of 95% confidence level.

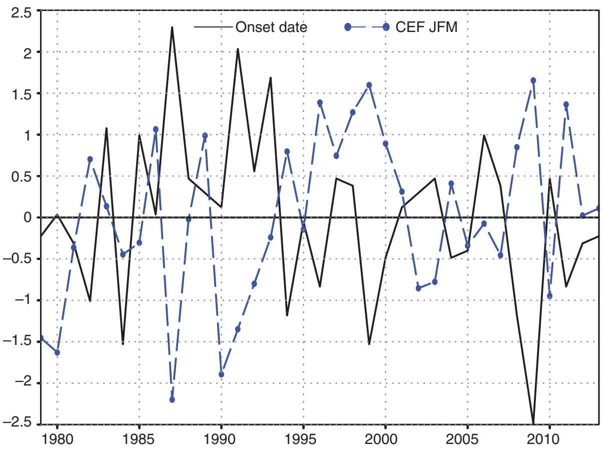

Figure 2. Standardized SCSSM onset date anomalies (line) and composite intensity anomalies of CEF from January to March nearby the Philippines (dashed line).

seasonal reversal from northerlies to southerlies nearby the Philippines occurs at 22 April for the past 35 years. Therefore, a positive (negative) CEF anomalies from January to March indicates a weakened (strengthened) climatological northerly winds around equator nearby the Philippines, and thus corresponds to a strong (weak) CEF.

4. Physical process by which the CEF affects SCSSM onset

4.1. Atmospheric circulations

Figure 3 shows the difference of 850 hPa winds and OLR between the years of positive and negative CEF anomalies. There is a cyclonic anomaly accompanied with reinforced convection over South China Sea and western North Pacific from January to March (Figures 3(a)–(c)). Easterly anomalies exist over equatorial Pacific and convection weakens over central equatorial Pacific. Obviously, from January to March the southerly anomalies is nearby the Philippines and the CEF is strengthened. The southerly anomalies in January and February is stronger than those in March, which is possibly due to the stronger convection over northern of equator. In April, cyclonic anomaly over South China Sea and western Pacific preserves, and the centre of convection is located over central and north region of South China Sea (Figure 3(d)). Convection over central and northern South China Sea enhances in April. Figure 4 shows the distribution of correlation coefficients between the date of SCSSM onset and vorticity at 850 hPa in April. By using vorticity averaged over northern South China Sea (110°–120°E,10°–20°N) to denote the intensity of South China Sea high, correlation analysis shows that the correlation coefficients between the intensity of South China Sea high in April and the composite CEF nearby the Philippines during January, February, and March is 0.4, which exceeds 98% confidence level. This result illustrates that the strong (weak) CEF nearby the Philippines in preceding months during January, February, and March is likely to be followed by a weakened (strengthened) subtropical high over South China Sea and western North Pacific in April.

Previous studies have demonstrated that the SCSSM onset is accompanied with the retreating eastward of subtropical high over western North Pacific (Ding *et al.*, 2004; Huang *et al.*, 2006; Kajikawa and Wang, 2012). It can be seen from Figure 4 that the negative correlation is significant over northern South China Sea and western North Pacific. An early (late) onset of SCSSM corresponds to a weak and eastward shifted (strong and westward shifted) subtropical high over South China Sea and western North Pacific, indicating that activity of subtropical high over South China Sea and western North Pacific in April is related closely with SCSSM onset.

The above analyses suggest that the subtropical high over South China Sea and western North Pacific in April may be a linkage of CEF nearby the Philippines in preceding months with SCSSM onset. A weak and eastward shifted (strong and westward shifted) subtropical high over South China Sea and western North Pacific in April corresponds to a strong (weak) CEF nearby the Philippines in preceding months from January to March, thereby results in an early (late) onset of SCSSM. However, what cause the anomalous CEF nearby the Philippines? What is the physical process linking the CEF nearby the Philippines in preceding months with the subsequent subtropical high over South China Sea and western North Pacific? In the following, these issues will be explored.

4.2. The role of SSTA

As shown in Figure 3, a cyclonic (anticyclonic) anomaly accompanied with reinforced (weakened) convection exists over South China Sea and western North Pacific when the CEF nearby the Philippines from January to March is strong (weak). Such circulation anomaly maintains from January to April. Previous research indicated that cyclonic (anticyclonic) circulation anomaly over South China Sea and western North Pacific in winter and spring is related closely with SSTA in tropical western Pacific (Zhang *et al.*, 1996, 1999; Zhang and Sumi, 2002; Zhang *et al.*, 2015). So it is necessary to investigate the role played by the SSTA in CEF anomalies. As shown

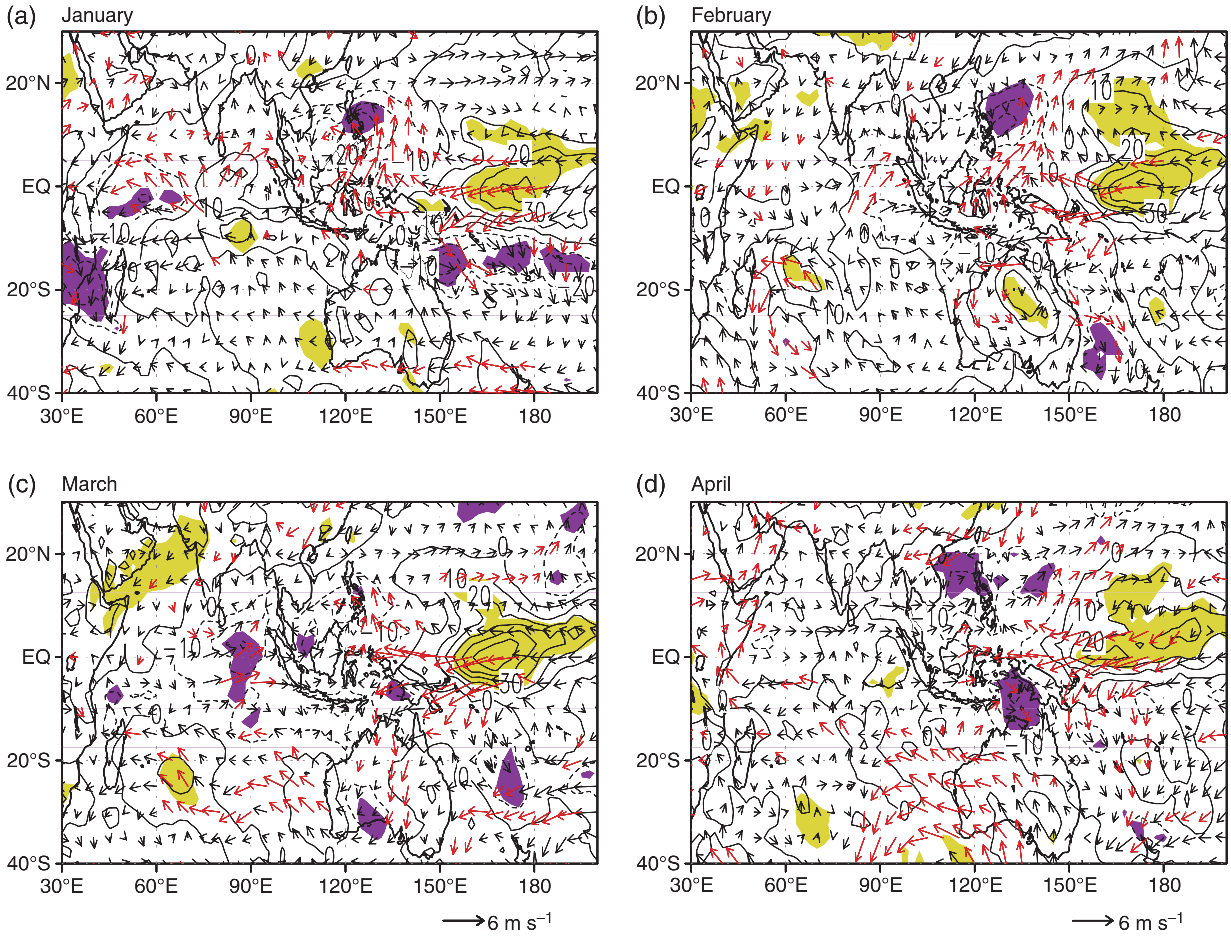

Figure 3. Difference of OLR (contour) and 850 hPa winds (vector) in (a) January, (b) February, (c) March, and (d) April between the years of positive and negative CEF anomalies nearby the Philippines. Shadings and red vectors represent OLR and winds passing 95% confidence level.

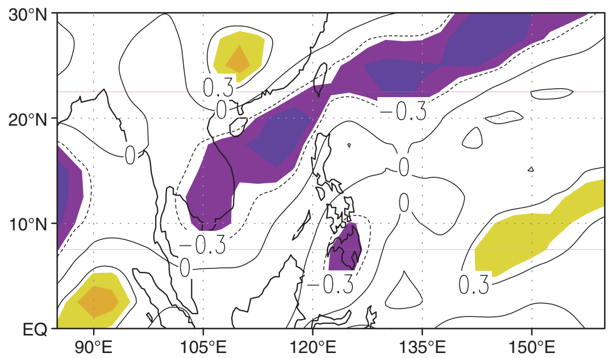

Figure 4. Correlation coefficients between the date of SCSSM onset and 850 hPa vorticity in April. Yellow and purple coloured areas indicate positive and negative coefficients passing 95% confidence level, respectively.

in Figure 5, there is positive SSTA to the north of the Equator in tropical western Pacific, which develops from preceding autumn, reaches the strongest in January and February, and decays in spring. It is worth to point out that the strong positive SSTA appears to the north of equator in western Pacific (120°–150°E). Because of the higher SSTA, strong convection is stimulated in the region around South China Sea and western North Pacific, resulting in reinforced CEF from south to north at these longitudes. It is thus clear that the CEF nearby the Philippines is enhanced (decayed) during the years of positive (negative) SSTA in South China Sea and western North Pacific due to the strengthened (weakened) convection over there. In tropics, the air temperature at lower troposphere is related closely with SSTA. During boreal winter and spring, atmospheric temperature at lower layer is influenced by ocean to a great extent. Figure 6(a) shows the significant positive atmospheric temperature at lower troposphere (including three layers of 1000, 925, and 850 hPa) over South China Sea and tropical western North Pacific, which means that the atmospheric temperature at lower layer rises (decreases) when SST rises (decreases). It can be also seen in Figure 6(a) that the atmospheric temperature to the south of equator along the longitudes of 120°–150°E does not significantly increase, implying a temperature gradient from south to north appears, and therefore resulting in the positive anomaly of CEF from south to north nearby the Philippines. This is another reason for the formation of CEF anomalies nearby the Philippines.

Previous studies have revealed that the cause of climatological CEF is associated with the seasonal transition of atmospheric circulation due to thermodynamic difference between Southern and Northern Hemisphere (Sashegyi

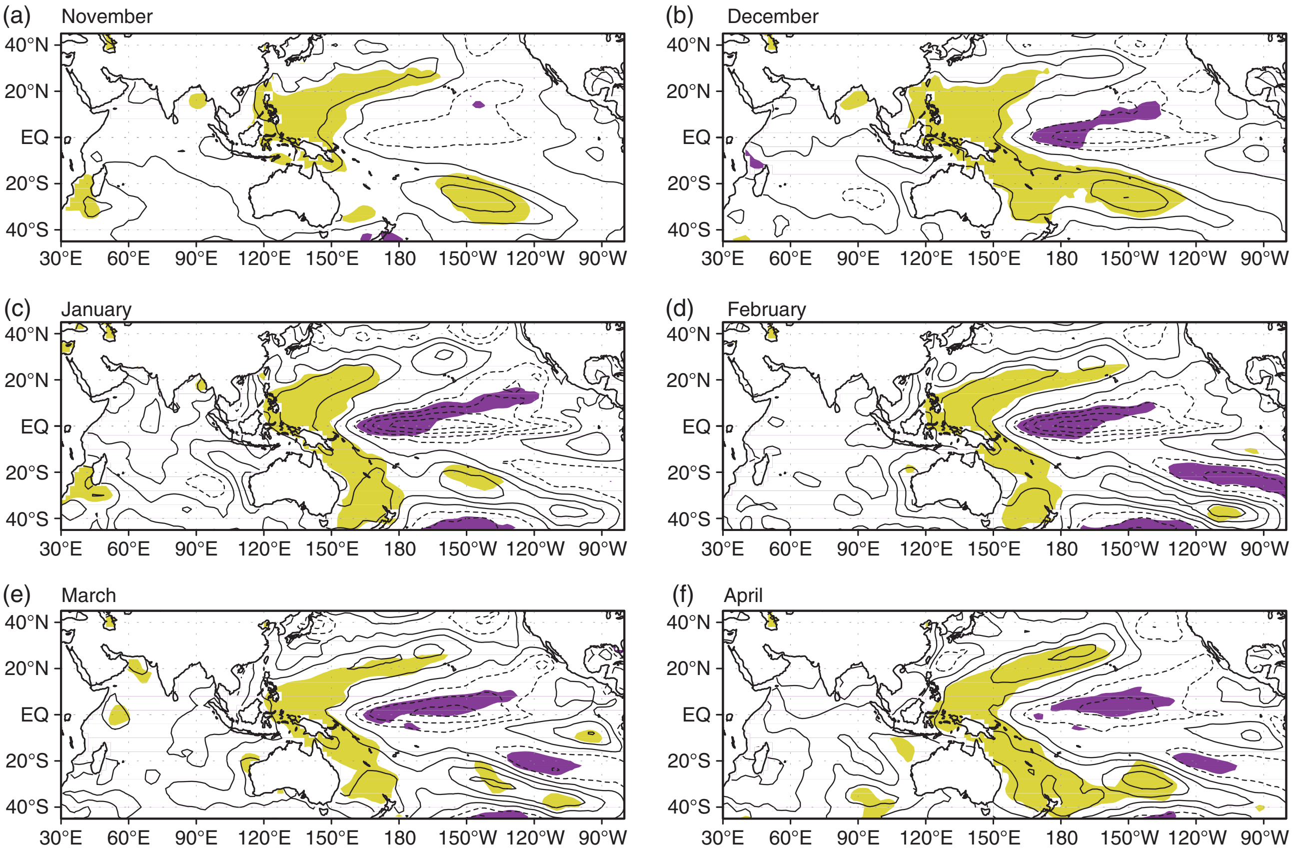

Figure 5. Difference of SSTA in (a) November, (b) December, (c) January, (d) February, (e) March, and April (f) between positive and negative anomalies of composite intensity of CEF nearby the Philippines from January to March. The contour interval is 0.3, yellow and purple coloured areas represent positive and negative anomalies passing 95% confidence level, respectively.

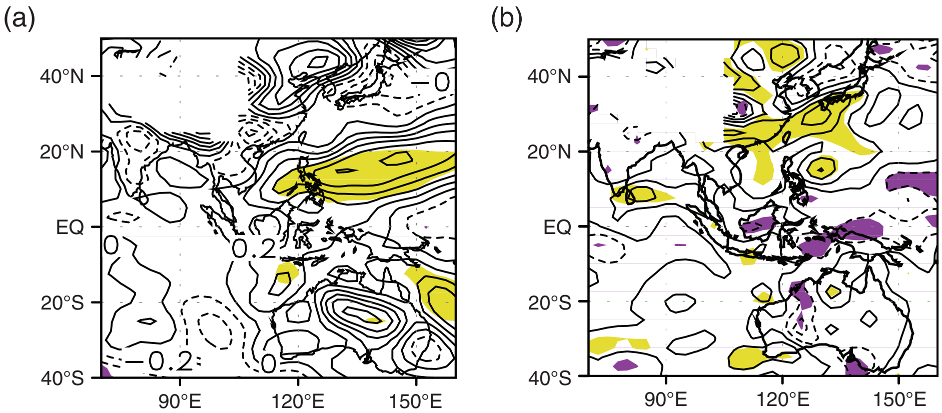

Figure 6. Differences of lower troposphere (a) temperature (unit: K) and (b) heating rate (unit: K s^{-1}) between strong and weak composite intensity of CEF nearby the Philippines from January to March. Yellow and purple coloured areas indicate positive and negative anomalies passing 95% confidence level, respectively.

and Geisler, 1987; Wang and Liao, 1997; Zeng and Li, 2002). In the following we are going to check the atmospheric apparent heat source that depicts diabatic heating in the years of strong (1986, 1996, 1998, 1999, 2009, 2011) and weak (1979, 1980, 1987, 1990, 1991) CEF nearby the Philippines from January to March.

Figure 6(b) gives the difference of averaged 1000, 925, and 850 hPa heating rate between strong and weak composite intensity of CEF nearby the Philippines from January to March. It is shown that in Asia-Australia monsoon region, diabatic heat anomalies are mainly positive over most areas of East Asia, South China Sea, and western North Pacific, and negative over maritime continent, equatorial western Pacific, and Australia. Such distribution of lower tropospheric heating rate anomalies forms a thermal gradient from south to north, and results in the strengthening of CEF from south to north nearby the Philippines. It is indicated that the anomaly of CEF nearby the Philippines is the respond to the anomalous distribution of atmospheric heating source. Combining the analyses in subsection 4.1, it is illustrated that the anomaly of CEF nearby the Philippines in January, February, and March is influenced jointly by both external forcing factors of underlying SSTA and atmospheric heating source corresponding to SSTA.

It is worth to point out that the atmospheric temperature anomalies in lower troposphere over South China Sea and western North Pacific in April is not statistically significant (Figure 7) although the anomalous pattern of SSTA in April is similar to that in preceding months from January to March. Therefore, the CEF anomaly nearby the Philippines is not obvious in April (Figure 3(d)). This is possibly related to the background of the climatological seasonal circulation. Climatologically, strong convection of Asia-Australia monsoon is located to the south of equator during the months of January, February, and March. In the same time, the region of South China Sea and western North Pacific is controlled by the belt of subtropical high which is not favourable for the developing of convection, and is basically a no convection zone. Solar radiation heats the sea surface directly and the variability of lower tropospheric atmosphere temperature is influenced to a great extent by thermal condition of underlying ocean. Therefore, positive (negative) SSTA corresponds to the positive (negative) temperature anomaly of lower troposphere over South China Sea and western North Pacific in these months on the whole. In April, convection belt of Asia-Australia monsoon moves northward to some extent, and shows a symmetrical distribution to the equator in general. The belt of subtropical high breaks over Indochina Peninsular in April (He *et al.*, 1997), convection enhances somewhat over South China Sea and western North Pacific. Consequently, convection anomaly over this region may impact on the solar radiation reaching sea surface and the SSTA may not be positively correlated with the lower tropospheric atmosphere temperature as those in January–March. It is thus evident that the atmospheric temperature of lower troposphere over South China Sea and western North Pacific in April is influenced by multiple factors, and does not corresponds directly to underlying SST.

How does the CEF anomaly nearby the Philippines in preceding months from January to March link with subtropical high over South China Sea and western North Pacific in April? Above analyses indicate that during the years of strong CEF nearby the Philippines in January, February, and March, the centres of cyclonic circulation and convection anomalies are located to the east of the Philippines, but move westward to northern South China Sea in April (Figure 3). The cyclonic circulation anomaly over northern South China Sea weakens the subtropical high over there and shifts it eastward, resulting in the early onset of SCSSM. But what cause the cyclonic circulation and convection anomalies moving to northern South China Sea in April? As seen in Figure 3, the cyclonic circulation and convection anomalies to the east of Philippine develop in January and reach the strongest

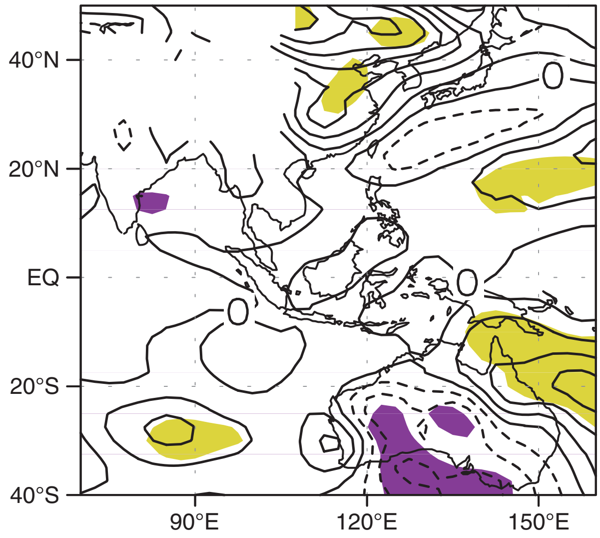

Figure 7. Difference of lower tropospheric temperature in April between strong and weak composite intensity of CEF nearby the Philippines from January to March. Contour interval is 0.5 K. Yellow and purple coloured areas indicate positive and negative anomalies passing 95% confidence level, respectively.

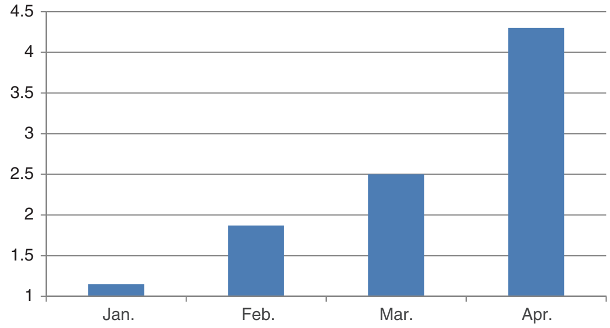

Figure 8. Climatological daily precipitation (mm) averaged over South China and northern South China Sea (110°–120°E,17°–25°N) in the months from January to April based on CMAP data in the period 1979–2014.

in February, and decay in March and April. The evolution characteristics of cyclonic circulation and convection anomalies to the east of Philippine correspond to the variation of SSTA in tropical western Pacific. The positive SSTA in tropical western Pacific (west of 150°E) is large in January and February, and becomes small in March and April (Figure 5). Then, why can cyclonic circulation and convection anomalies over northern South China Sea in April develop in the condition of weakened SSTA?

From climatological aspect, precipitation over costal South China begins to increase in April (Lin *et al.*, 2010). As shown in Figure 8, climatological precipitation over South China and northern South China Sea increases dramatically in April compared to that in March. Figure 9 shows the climatological water vapour flux at 850 hPa and outgoing long-wave radiation (OLR) in March and April, respectively. It can be seen that the area of OLR larger than 260 W m^{-2} which depicts subtropical high exhibits a long belt across subtropical region from Western Pacific

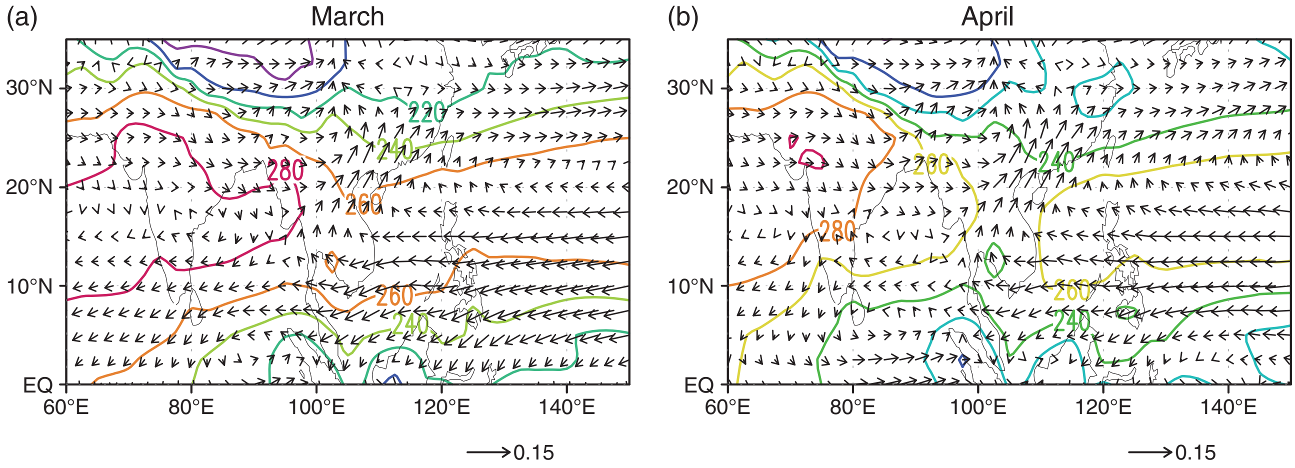

Figure 9. Climatological monthly water vapour flux at 850 hPa (vectors; unit: 10 kg hPa^{-1} m^{-1} s^{-1}) and OLR (contours; unit: W m^{-2}) in (a) March and (b) April.

to the Arabia Sea in March. Subtropical high breaks over Indochina Peninsular in April, resulting in the increasing of water vapour flux over northern South China Sea and costal South China along the western edge of western North Pacific subtropical high. Thus the precipitation in April over the region is much more than that in March. It is clear that the climatological states of atmospheric humidity and thermal condition in April are different evidently from those in March. It seems that, despite the weakening of positive SSTA, the changes in climatological basic conditions in April are conducive to the developing of convection over northern South China Sea, which favours the early onset of SCSSM.

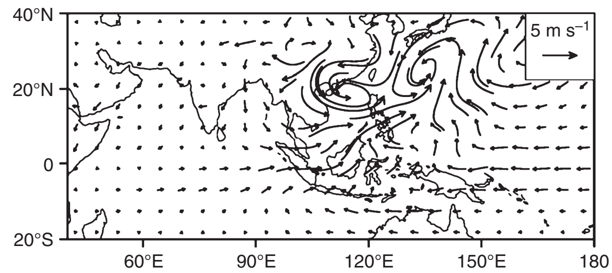

Figure 10. Wind field at 850 hPa in response to the atmospheric heating over South China sea and western North Pacific (110°–140°E, 10°–25°N) simulated by GFDL dry model.

4.3. Numerical experiments

According to above observational analyses, we argue that the CEF nearby the Philippines in preceding months from January to March links the SCSSM onset through affecting the subtropical high over South China Sea and western North Pacific in April. The basic causes in the relationship between the CEF nearby the Philippines and the subsequent subtropical high are the atmospheric heating source and SSTA. To confirm the results based on observational analyses, GFDL_dry and CAM4 models are utilized.

To mimic the observed vertical profile of sensible heating, the anomalous heating rate of 10 times of the composite shown in Figure 6 is prescribed at the lowest level ($\sigma = 0.9$) in the GFDL_dry model over South China Sea and western North Pacific (10°–25°N, 110°–140°E). Multiplication of the heating anomaly by a factor of 10 is for obtaining a stronger and more robust model response. As shown in Figure 10, the simulated wind response is similar to observations. There is a cyclonic circulation over northern South China Sea and western North Pacific at 850 hPa, and CEF from south to north nearby the Philippines (120°–130°E) appears. The numerical experiment of GFDL_dry model corroborates that the atmospheric heating source over South China Sea and western North Pacific results in the simultaneous CEF anomaly nearby the Philippines and the circulation anomaly over northern South China Sea and western North Pacific.

Figure 5 shows that the SSTA in central Pacific is also significant in addition to the tropical western Pacific. To examine the role played by the SSTA in central Pacific, a control run experiment (CTL) and two sets of sensitivity experiments are designed by using the CAM4 model, and each experiment performs a 30-year integration. The CTL is forced by the climatological annual cycles of SST and sea ice concentration. The first sensitivity experiment is constructed by adding the composite SSTA from Figure 5 in central Pacific onto the climatological SST, and the second one by adding only the SSTA in western Pacific. The last 25 years of each experiment are selected to analyse. The difference between sensitivity experiment and CTL is used to analyse the response of atmospheric circulation to the SSTA in different region in tropical Pacific from January to April. Figure 11 shows the composite difference for the last 25 years between first sensitivity experiment and CTL. It can be seen that the CEF nearby the Philippines does not enhance in winter and spring. As a response to the cold anomalies in central equatorial Pacific, the easterly winds prevail over western equatorial Pacific. But the difference between the second sensitivity experiment and CTL (Figure 12) shows the similar characteristics to the observations. The warm SSTA in tropical western Pacific

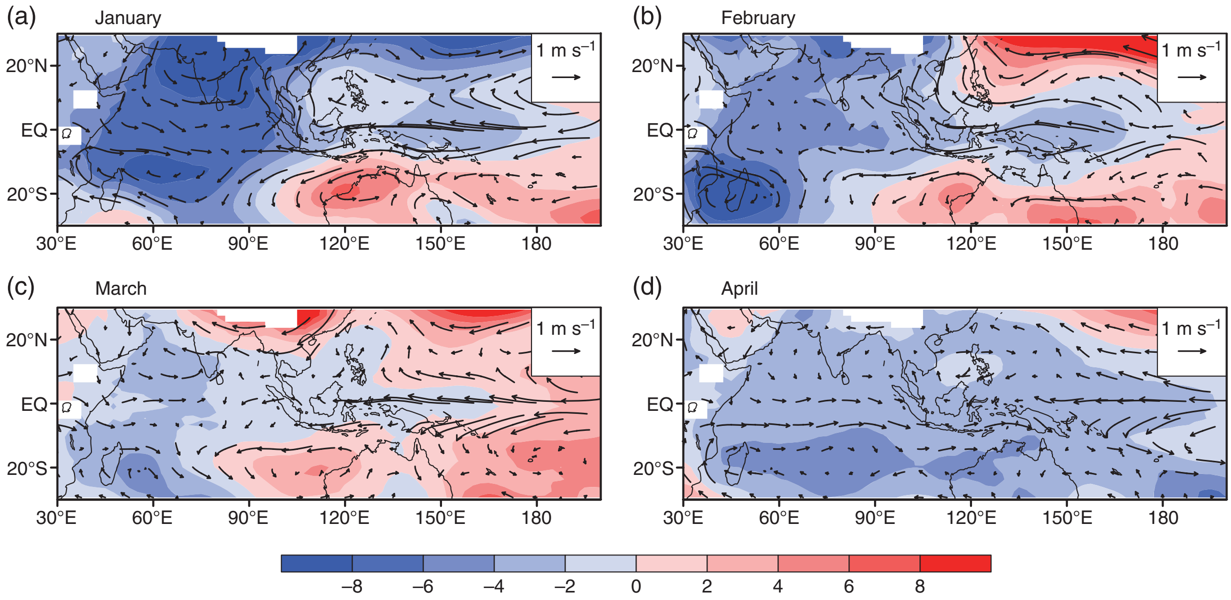

Figure 11. Difference of geopotential heights (shadings) and winds (vectors) at 850 hPa between first sensitivity experiment and CTL simulated by CAM4 model.

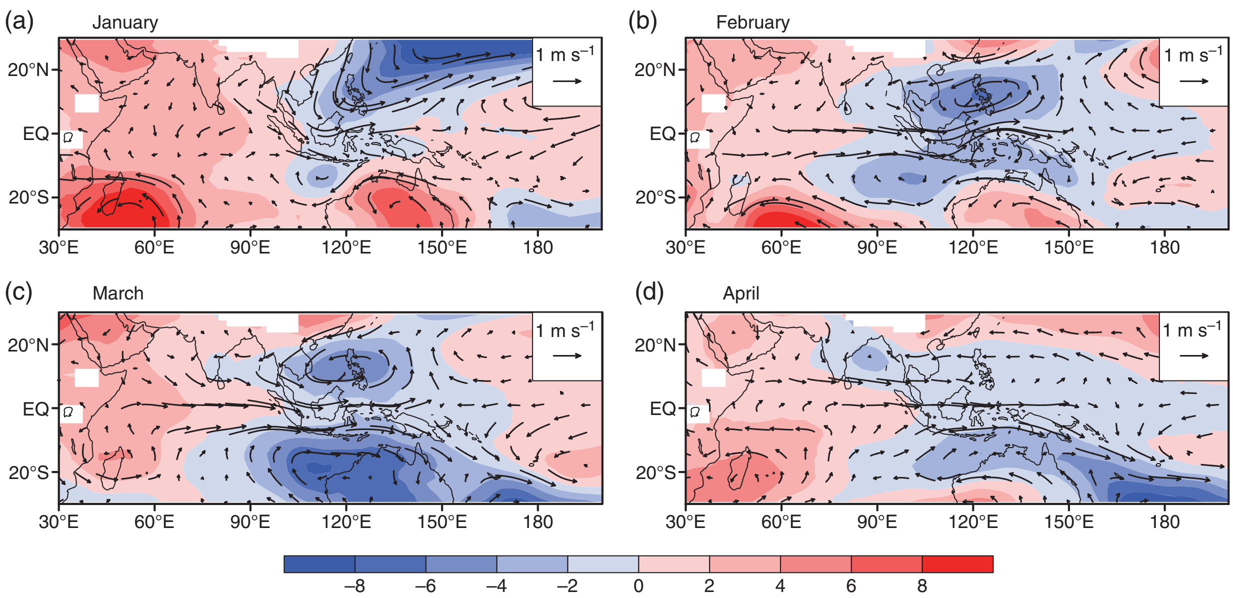

Figure 12. Same as Figure 11 but between the second sensitivity experiment and CTL.

results in the strong CEF nearby the Philippines in January, February, and March as well as weak subtropical high over South China Sea and western North Pacific in April. Actually, recent research has shown that warm SSTA in tropical western Pacific associated with ENSO plays an important role in affecting the circulations over East Asia and western North Pacific (Zhang *et al.*, 2015).

Based on the results of observation analyses and numerical experiments, the external forcing on CEF anomalies nearby the Philippines in preceding months is the atmospheric diabatic heating over Asian-Australian monsoon region and SSTA over tropical western Pacific. SSTA in tropical western Pacific along with the climatological atmospheric background over northern South China Sea and coastal South China in April result together in the anomaly of subtropical high over northern South China Sea and western North Pacific, and thus impact on the SCSSM onset.

5. Conclusion and discussion

The relationship between CEF nearby the Philippines from winter to spring and the SCSSM onset is investigated by using observation analyses and numerical experiments. It is found that the date of SCSSM onset has a significant negative correlation with the CEF nearby the Philippines in preceding months from January to March, namely, a strong CEF nearby the Philippines during January, February, and

March tends to be succeeded by an early onset of SCSSM, whereas a weak CEF is likely to be followed by a late onset of SCSSM.

The CEF in preceding months is related closely with subtropical high over South China Sea and western North Pacific in April, through which the CEF in preceding months links the SCSSM onset. The subtropical high in April is weak and eastward shifted (strong and westward shifted) in the years when the CEF in January, February, and March is strong (weak). The weak and eastward shifted (strong and westward shifted) subtropical high favours (does not favour) the convection developing over northern South China Sea, then the onset of SCSSM is early (late).

The basic causes of close relationship between anomalies of CEF nearby the Philippines in preceding months and subtropical high in April over South China Sea and western North Pacific are the effects of SSTA and anomalous atmospheric heating source over tropical western Pacific. SSTA in tropical western Pacific, on the one hand, results in the anomalies of CEF nearby the Philippines in January, February, and March, and, on the other hand, influences the subtropical high in April. The positive SSTA in tropical western Pacific and the wet and warm climatic background over northern South China Sea and Coastal areas of Southern China in April impact together the abnormal activity of subtropical high over South China Sea and western North Pacific.

Previous studies have demonstrated that the onset of SCSSM has a decadal shift occurred around 1993/1994 (Kwon *et al.*, 2005; Kajikawa and Wang, 2012; Lin *et al.*, 2013). To check the effect of the decadal shift on our results, we calculated the correlation coefficients between the CEF and the onset of SCSSM in the periods of 1979–1993 and 1994–2013, which are −0.33 and −0.69, respectively. Same as the correlation coefficient in the period of 1979–2013, the correlation coefficients in both sub-periods are negative. However, the correlation coefficient in the last period is much higher and exceeds the 0.01 confidence level, and that in the first period fails in passing the 0.05 confidence level. Therefore, although in the total period of 1979–2013 our results are robust, the relationship between the CEF and SCSSM onset revealed in the present study seems being affected by the decadal shift and becomes more prominent after the decadal shift in 1993/1994. The effect of the decadal shift on the relationship between the CEF and SCSSM onset is an important topic for our future study. This study only focuses at the interannual timescale. Actually, atmospheric intraseasonal oscillation modulates monsoon onset as well (Hendon and Liebmann, 1990; Lin, 1998; Mu and Li, 2000; Wen *et al.*, 2006; Lin *et al.*, 2016). Therefore, how CEF at intraseasonal scale cooperated with interannual variation impact SCSSM onset is worth to investigate further. In addition, the study on the interaction between atmospheric heating and SSTA over tropical western Pacific mentioned hereinbefore is needed in the future.

Acknowledgements

This research was supported by the National Program on Key Basic Research Project (2014CB953901), National Key Research and Development Program (2016YFA0600602) and the National Natural Science Foundation of China under Grants 41575043 and 41661144017.

References

Bi B, Zhang G, Li Z. 2004. The relationship of abnormal features of western Pacific subtropical high and 2003 Huaihe River flood and cause exploration. *J. Trop. Meteorol.* **20**: 505–514 (in Chinese).
Chen L, Li W, Zhao P, Tao S. 2000. On process of Summer Monsoon onset over East Asia. *Clim. Environ. Res.* **5**: 345–355. https://doi.org/10.3878/j.issn.1006-9585.2000.04.02 (in Chinese).
Ding Y, He C. 2006. The summer monsoon onset over the tropical eastern Indian Ocean: the earliest onset process of the Asian summer monsoon. *Adv. Atmos. Sci.* **23**: 940–950.
Ding Y, Li C. 1999. *Onset and evolution of the South China Sea monsoon and its interaction with the ocean*. China Meteorological Press: Beijing, China.
Ding Y, Li C, Liu Y, Zhang J, Song Y. 2002. South China Sea monsoon experiment. *Clim. Environ. Res.* **7**: 202–208 (in Chinese).
Ding Y, Li C, Liu Y. 2004. Overview of the South China Sea monsoon experiment. *Adv. Atmos. Sci.* **21**: 343–360.
Feng T, Shen X, Huang R, Chen G. 2014. Influence of the interannual variation of cross-equatorial flow on tropical cyclogenesis over the western north Pacific. *J. Trop. Meteorol* **30**: 11–22 (in Chinese).
Findlater J. 1969. A major low-level air current near the Indian Ocean during the northern summer. *Quart. J. R. Meteorol. Soc.* **95**: 362–380.
Gao H, Xue F. 2006. Seasonal variation of the cross-equatorial flows and their influences on the onset of South China Sea summer monsoon. *Clim. Environ. Res.* **11**: 57–68 (in Chinese).
He J, Chen L. 1989. Quasi-40 day oscillations over the mid-latitude of the Southern Hemisphere with their relation to the summer monsoon over the Northern Hemisphere. *J. Nanjing Inst. Meteorol.* **12**: 11–18 (in Chinese).
He J, Li J, Li Y. 1991. Numerical experiment with processes for effect of Australian cold air activity on East Asian summer monsoon. *Acta. Meteor. Sin.* **49**(2): 162–169 (in Chinese).
He J, Zhu Q, Murakami M. 1997. T_{bb} data-revealed features of Asian-Australian monsoon seasonal transition and Asian summer monsoon establishment. *J. Trop. Meteorol.* **3**: 18–26.
Hendon H, Liebmann B. 1990. A composite study of the onset of the Australian summer monsoon. *J. Atmos. Sci.* **47**: 2227–2240.
Huang R, Gu L, Zhou L, Wu S. 2006. Impact of the thermal state of the tropical western Pacific on onset date and process of the South China Sea summer monsoon. *Adv. Atmos. Sci.* **23**: 909–924.
Huang Y, Li C, Wang Y. 2008. Study on the causation of anomaly of cyclogenesis frequency and location of tropical cyclones over the western north Pacific in 2006. *J. Trop. Meteorol.* **24**: 590–598 (in Chinese).
Hurrell JW, Hack JJ, Shea D, Caron JM, Rosinski J. 2008. A new sea surface temperature and sea ice boundary dataset for the community atmosphere model. *J. Clim.* **21**: 5145–5153. https://doi.org/10.1175/2008jcli2292.1.
Jiang X, Li T. 2005. Reinitiation of the Boreal summer intraseasonal oscillation in the tropical Indian Ocean. *J. Clim.* **18**: 3777–3795. https://doi.org/10.1175/jcli3516.1.
Kajikawa Y, Wang B. 2012. Interdecadal change of the South China Sea summer monsoon onset. *J. Clim.* **25**: 3207–3218.
Kanamitsu M, Ebisuzaki W, Woollen J, Yang S-K, Hnilo JJ, Fiorino M, Potter GL. 2002. NCEP–DOE AMIP-II Reanalysis (R-2). *Bull. Am. Meteorol. Soc.* **83**: 1631–1643.
Krishnamurti TN, Molinari J, Pan HL. 1976. Numerical-simulation of Somali Jet. *J. Atmos. Sci.* **33**: 2350–2362.
Kuettner JP, Unninayar MS. 1980. The near equatorial jet of southern India and its role in the onset of the monsoon. Results of Summer MONEX Field Phase Research (Part B), FGGE Operations Report 9, WMO.
Kwon M, Jhun J-G, Wang B, An S-I, Kug J-S. 2005. Decadal change in relationship between East Asian and WNP summer monsoons. *Geophys. Res. Lett.* **32**: L16709. https://doi.org/10.1029/2005gl023026.

Lei X, Yang X. 2008. Interannual variation characteristics of east hemispheric cross-equatorial flow and its contemporaneous relationships with temperature and rainfall in China. *J. Trop. Meteorol.* **24**: 127–135 (in Chinese).

Leung MYT, Cheung HHN, Zhou W. 2016. Meridional displacement of the East Asian trough and its response to the ENSO forcing. *Clim. Dyn.* **45**: 1–18. https://doi.org/10.1007/s00382-016-3077-8.

Li C, Li S. 2014. Interannual seesaw between the Somali and the Australian Cross-Equatorial flows and its connection to the East Asian summer monsoon. *J. Clim.* **27**: 3966–3981.

Li C, Wu J. 2002. Important role of the Somalian cross-equator flow in the onset of the South China Sea summer monsoon. *Chin. J. Atmos. Sci.* **26**(2): 185–192 (in Chinese).

Li Z, Qian C, Sun C. 2000. A priliminary analysis on the relationship between the cross-equatorial flow and the heavy rainfall over Yangtze and Huaihe river in 1991. *Acta. Meteor. Sin.* **58**: 628–636 (in Chinese).

Liang Z, Wen Z, Wu L. 2006. The relationship between the Indian Ocean sea surface temperature anomaly and the onset of South China Sea summer monsoon I. coupling analysis. *Chin. J. Atmos. Sci.* **30**: 619–634 (in Chinese).

Lin A. 1998. The characteristics of low-frequency oscillations over the South China Sea. *J. Trop. Meteorol.* **4**(2): 141–147.

Lin X, Xu J, Wen Z, He F, Chi Y. 2007. Variation features of Somali cross-equatorial flow and its impact on the location of the subtropical high ridge from July to September. *J. Trop. Meteorol.* **23**: 505–509 (in Chinese).

Lin A, Li C, Zheng B, Gu D, Liang J. 2010. Relationship between onset of South China Sea summer monsoon and South China frontal precipitation in the first raining period on climatological mean. *Acta Scientiarum Naturalium Universitatis Sunyatseni* **49**(4): 134–143 (in Chinese).

Lin A, Gu D, Zheng B, Li C. 2013. Relationship between South China Sea summer monsoon onset and Southern Ocean sea surface temperature variation. *Chin. J. Geophys.* **56**: 383–391. https://doi.org/10.6038/cjg20130203 (in Chinese).

Lin A, Gu D, Li C, Zheng B. 2016. Impact of equatorial MJO on South China Sea summer monsoon onset. *Chin. J. Geophys.* **59**(1): 28–44. https://doi.org/10.6038/cjg20160104 (in Chinese).

Liu X, Sun Z, Li W, Huang L. 2009. The circulation configuration of strong/ weak cross-equatorial flow to the north of Australia. *Chin. J. Atmos. Sci.* **33**: 1348–1362 (in Chinese).

Mao J, Xie A, Song Y, Ye Q. 2000. Impact of sea surface temperature and its variations on the onset of summer monsoon over South China Sea. *Acta. Meteor. Sin.* **58**: 556–569 (in Chinese).

Mu M, Li C. 2000. On the outbreak of South China Sea summer monsoon in 1998 and activity of atmospheric intraseasonal oscillation. *Clim. Environ. Res.* **5**: 375–387. https://doi.org/10.3878/j.issn.1006-9585.2000.04.05 (in Chinese).

Neale RB, Richter JH, Conley AJ, Park S, Lauritzen PH, Gettelman A, Williamson DL, Rasch PJ, Vavrus SJ, Taylor MA, Collins WD, Zhang MH, Lin S-J. 2010. Description of the NCAR Community Atmosphere Model (CAM4.0), USA.

Qian Y, Wang Q, Dong Y, Gong Y. 1987. Numerical experiment of Somali jet. *Chin. J. Atmos. Sci.* **11**: 176–184 (in Chinese).

Qiu J, Sun Z. 2013. Variation characteristics of the vertical structure of the summer Somali cross-equatorial flow and its relationship with East Asia summer monsoon activity. *Chin. J. Atmos. Sci.* **37**: 1129–1142 (in Chinese).

Ramaswamy C, Pareek RS. 1978. The southwest monsoon over Indian and its teleconnections with the middle and upper tropospheric flow patterns over the Southern Hemisphere. *Tellus* **30**: 126–135.

Rodwell MJ. 1997. Breaks in the Asian monsoon: the influence of southern hemisphere weather systems. *J. Atmos. Sci.* **54**: 2597–2611.

Rodwell MJ, Hoskins BJ. 1995. A model of the Asian summer monsoon. 2. Cross-equatorial flow and Pv behavior. *J. Atmos. Sci.* **52**: 1341–1356.

Sashegyi KD, Geisler JE. 1987. A linear model study of cross-equatorial flow forced by summer monsoon heat sources. *J. Atmos. Sci.* **44**: 1706–1722.

Sikka DR. 1980. Southern Hemisphere influences and the onset of the southwest monsoon of 1979. Results of Summer MONEX Field Phase Research (Part B). FGGE Operations Report 9, WMO.

Smith T, Reynolds R. 2004. Improved extended reconstruction of SST (1854–1997). *J. Clim.* **17**: 2466–2477.

Tang M, Huang S, Zhou D. 1985. On the spatial and temporal variation of the cross-equatorial currents around the globe. *J. Trop. Meteorol.* **1**: 287–296 (in Chinese).

Tao S, He S, Yang Z. 1983. An observational study on the onset of the summer monsoon over Eastern Asia in 1979. *Chin. J. Atmos. Sci.* **7**: 347–355 (in Chinese).

Wang H, Fu R. 2002. Cross-equatorial flow and seasonal cycle of precipitation over South America. *J. Clim.* **15**: 1591–1608.

Wang J, Leftwich PW. 1984. A major low-level cross-equatorial current at 110oE during the northern summer and its relation to typhoon activities. *Chin. J. Atmos. Sci.* **8**: 443–449. https://doi.org/10.3878/j.issn.1006-9895.1984.04.11 (in Chinese).

Wang and Liao. 1997. On the effects of heat forcing upon the formation and maintenance of the cross equatorial flow-qualitative analysis. *Acta Meteor. Sin.* **55**: 484–491 (in Chinese).

Wang H, Xue F. 2003. Interannual variability of Somali jet and its influences on the inter-hemispheric water vapor transport and on the East Asian summer rainfall. *Chin. J. Geophys.* **46**: 18–25 (in Chinese).

Wang L, Li T, Zhou T. 2012. Intraseasonal SST Variability and Air-Sea Interaction over the Kuroshio Extension Region during Boreal Summer. *J. Clim.* **25**: 1619–1634. https://doi.org/10.1175/jcli-d-11-00109.1.

Wei W, Zhang R, Wen M, Rong X, Li T. 2014. Impact of Indian summer monsoon on the South Asian high and its influence on summer rainfall over China. *Clim. Dyn.* **43**: 1257–1269.

Wei W, Zhang R, Wen M, Kim B-J, Nam J-C. 2015. Interannual variation of the South Asian High and its relation with Indian and East Asian summer monsoon rainfall. *J. Clim.* **28**: 2623–2634.

Wen Z, Huang R, He H, Lan G. 2006. The influences of anomalous atmospheric circulation over mid-high latitudes and the activities of 30–60 d low frequency convection over low latitudes on the onset of the South China Sea summer monsoon. *Chin. J. Atmos. Sci.* **30**: 952–964. https://doi.org/10.3878/j.issn.1006-9895.2006.05.23 (in Chinese).

Xu J, Wen Z, He F. 2006. Impact s of cross- equatorial flow on subtropical high ridge jumping northward to 25°N. *Meteorol. Mon.* **32**: 81–87 (in Chinese).

Yanai M, Esbensen S, Chu J. 1973. Determination of bulk properties of tropical cloud clusters from large scale heat and moisture budgets. *J. Atmos. Sci.* **30**: 611–627.

Zeng Q, Li J. 2002. Interactioins between the northem and southern hemispheric atmospheres and the essence of monsoon. *Chin. J. Atmos. Sci.* **26**(4): 433–448 (in Chinese).

Zeng G, Sun Z, Deng W, Lin Z, Li C. 2011. Numerical simulation of SSTA impacts upon the interdecadal variation of the cross-equator flows in eastern hemisphere. *J. Trop. Meteorol.* **27**: 609–618 (in Chinese).

Zhang R, Sumi A. 2002. Moisture circulation over East Asia during El Niño episode in northern winter, spring and autumn. *J. Meteorol. Soc. Jpn.* **80**: 213–227.

Zhang R, Sumi A, Kimoto M. 1996. Impact of El Niño on the East Asia monsoon: a diagnostic study of the ’86/87 and ’91/92 events. *J. Meteorol. Soc. Jpn.* **74**: 49–62.

Zhang R, Sumi A, Kimoto M. 1999. A diagnostic study of the impact of El Niño on the precipitation in China. *Adv. Atmos. Sci.* **16**: 229–241.

Zhang R, Li T, Wen M, Liu L. 2015. Role of intraseasonal oscillation in asymmetric impacts of El Niño and La Niña on the rainfall over southern China in boreal winter. *Clim. Dyn.* **45**: 559–567.

Zhao Y, Chen Y, Bai X, Wang F. 2000. The relations between the SST anomalies in South China Sea-Tropical Eastern Indian Ocean and the South China Sea monsoon. *J. Trop. Meteorol.* **16**: 115–123 (in Chinese).

Zhu Y. 2012. Variations of the summer Somali and Australia cross-equatorial flows and the implications for the Asian summer monsoon. *Adv. Atmos. Sci.* **29**: 509–518. https://doi.org/10.1007/s00376-011-1120-6.